Eidgenössische Technische Hochschule Zürich
Swiss Federal Institute of Technology Zurich

Autonomous Systems Laboratory

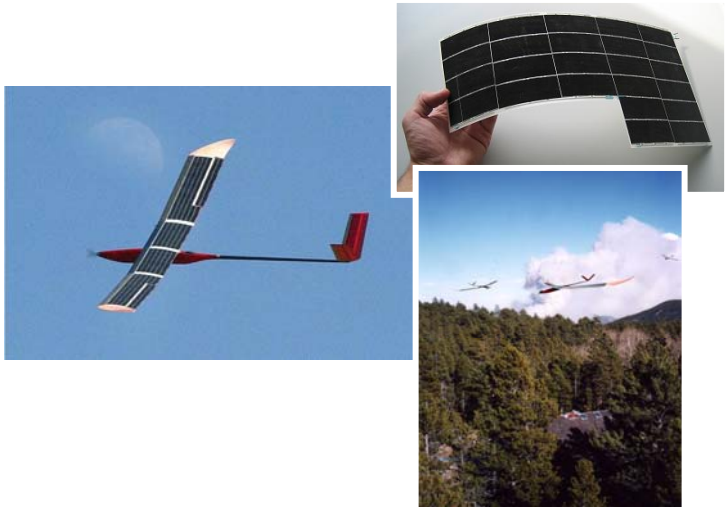

Design of Solar Powered Airplanes for Continuous Flight

given in the framework of the ETHZ lecture
"Aircraft and Spacecraft Systems: Design, Modeling and Control"

partially included of a forthcoming Springer book chapter on
"Advances in Unmanned Aerial Vehicles, State of the art and the road to autonomy"

A. Noth and R. Siegwart

Version 1.0

December 2006

1 Introduction

The achievement of a solar powered aircraft capable of continuous flight was still a dream some years ago, but this great challenge has become feasible today. In fact, significant progresses have been realized recently in the domains of flexible solar cells, high energy density batteries, miniaturized MEMS and CMOS sensors, and powerful processors.

The concept is quite simple; equipped with solar cells covering its wing, it retrieves energy from the sun in order to supply power to the propulsion system and the control electronics, and charge the battery with the surplus of energy. During the night, the only energy available comes from the battery, which discharges slowly until the next morning when a new cycle starts.

Nevertheless, major interdisciplinary effort is necessary to optimize and integrate concepts and technologies to a fully functional system. As a matter of fact, the major issue is the combination and sizing of the different parts in order to maximize a certain criterion, for example the endurance, one parameter being the embedded payload.

In 2004, the Autonomous Systems Lab of EPFL/ETHZ launched the Sky-Sailor project under a contract with the European Space Agency. The objectives are the study and realization of a solar aircraft fully autonomous in navigation and power generation flying on Earth and thus validate the feasibility of a Mars dedicated version.

This lecture presents the methodology used for the global design of solar powered airplanes that are intended to achieve continuous flight on Earth. It was applied to the first prototype of Sky-Sailor but it is rather general so that it can be used as much for small airplane weighing some hundreds of gram as for solar high altitude long endurance (HALE) platforms with a wingspan of several tens of meters.

1.1 History of Solar Flight

Premises of solar aviation with model airplanes

On the 4th of November 1974, the first flight of a solar-powered aircraft took place on the dry lake at Camp Irwin, California. *Sunrise I*, designed by R.J. Boucher from Astro Flight Inc. under a contract with ARPA, flew 20 minutes at an altitude of around 100 m during its inaugural flight. An improved version, Sunrise II, was built and tested on the 12th of September 1975. The new cells, with a higher efficiency of 14%, delivered a power of 600 W.

Sunrise II, 1975

In Europe, the pioneers of solar model airplane were Helmut Bruss and Fred Militky. On the 16th of August 1976, his model *Solaris* completed three flights of 150 seconds reaching the altitude of 50 m [3].

Since this early time, many model airplane builders tried to fly with solar energy, this hobby becoming more and more affordable. The endurance, limited to a few seconds at the beginning, rapidly became minutes and then hours... [3]. Some people distinguished themselves like Dave Beck with *Solar Solitude* in 1996, Wolfgang Schaeper who set many

records with *Solar Excel* in the 90's and Sieghard Dienlin with his tiny solar model *PicoSol* in 1998.

The dream of manned solar flight

Gossamer Penguin, 1980

After having flown solar model airplanes and proved that it was feasible with sufficient illumination conditions, the new challenge that fascinated the pioneers at the end of the 70's was solar manned flights.

The first models, *Solar One* of Fred To in GB and *Solar Riser* of Larry Mauro, used the concept was to charge a battery on the ground using their solar panels and then achieve short duration flights. The crucial stage consisting in flying with the single energy of the sun without any storage was reached by Dr. Paul B. MacCready and his company AeroVironment Inc in the US. On the 18th of May 1980, the *Gossamer Penguin* realized what can be considered as the world's first piloted, solar-powered flight. On July 7, 1981, the next version named *Solar Challenger* crossed the English Channel with solar energy as its sole power source.

In Germany, Günter Rochelt built *Solair I*, a 16 m wingspan solar airplane that incorporated a battery. On the 21st of August 1983 he flew, mostly on solar energy and also thermals, during 5 hours 41 minutes. In 1986, Eric Raymond started the design of the *Sunseeker* in the US. At the end of 1989, it was test flown as a glider and during August 1990, it crossed the United States in 21 solar-powered flights with 121 hours in the air.

In 1996, the Berblinger Contest took place in Ulm with the objective to develop a real, practically usable solar aircraft that should be able to stay up with at least half the solar energy a good summer day with clear sky can give. The team of Prof. Rudolf Voit-Nitschmann from Stuttgart University won the first prize with *Icaré 2*.

On the way to HALE (High Altitude Long Endurance) platforms and eternal flight

After the success of *Solar Challenger*, the US government gave funding to AeroVironment Inc. to study the feasibility of long duration, solar electric flight at high altitude. In 1993, the *Pathfinder*, with its 30 m wingspan and 254 kg, was tested at low altitude and became in 1994 part of NASA's Environmental Research Aircraft Sensor Technology (ERAST) program.

Helios, 1999-2003

From 1994 to 2003, this program led to the construction of a series of three successive solar aircrafts, *Pathfinder Plus*, *Centurion* and *Helios*. The latter was intended to be the ultimate "eternal airplane", incorporating energy storage for night-time flight. In 2001, *Helios* set an unofficial world record altitude of 29'524 m (96'863 ft) but unfortunately, it never proved sustainable flight as it was destroyed when it fell into the Pacific Ocean on June 26, 2003 due to structural failures.

In Europe, many projects were also conduced on HALE platforms. At the DLR Institute of Flight Systems, *Solitair* was developed within the scope of a study from 1994 to 1998 [23]. The *Helinet* project, funded by a European Program, ran between January 2000 and March

2003 with the target to study the feasibility of a solar-powered HALE platform for broadband communications and Earth observation.

QinetiQ, a British company, is also very active in the field of solar HALE platforms with *Zephyr*, an airplane which flew in July 2006 for 18 hours, including 7 hours of flying in the dark. It has recently been selected as the base platform for the Flemish HALE UAV remote sensing system *Mercator* in the framework of the Pegasus project. The platform should fulfill missions like forest fire monitoring, urban mapping, coastal monitoring, etc.

But the objective of *Helios* to prove the feasibility of eternal flight for an unmanned airplane was reached on the 22nd of April 2005. Alan Cocconi, president and founder of AcPropulsion, flew his *Solong* during 24 hours and 11 minutes using only solar energy coming from its solar panels and also thermals, currents of warm air rising from the desert floor. The 4.75 m wingspan and 11.5 kg airplane confirmed its capabilities two months later on the 3rd of June with a flight lasting 48 hours and 16 minutes.

The next dream to prove continuous flight with a pilot on board will perhaps come true with *Solar-Impulse*, a 80 m wingspan lightweight solar airplane built in Switzerland. After the manufacturing of a 60 m prototype in 2007-2008 and the final airplane in 2009-2010, a round-the-world flight should happen in May 2011 with a stopover on each continent.

1.2 Brief description of the principle

Solar panels, composed by solar cells connected in a certain configuration, cover a certain surface of wing or other part of the airplane (tail, fuselage,…). During the day, depending on the sun irradiance and the inclination of the rays, the convert light into electrical energy. A converter, called Maximum Power Point Tracker, ensures that the maximum amount of power is obtained from the solar panels. This power is used firstly to power the propulsion group and the onboard electronics, and secondly to charge the battery with surplus of energy.

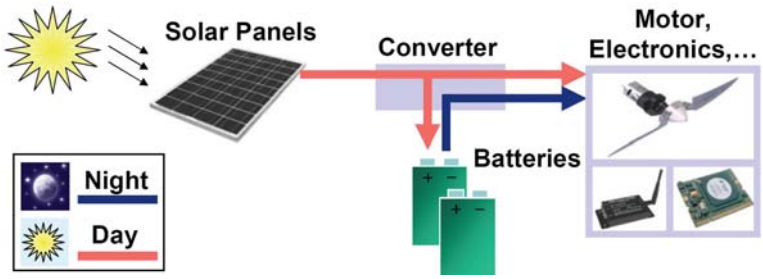

Fig. 1 Schematic representation of power transfer

During the night, as no more power comes from the solar panels, only the battery supplies the various elements. This is schematically represented on the figure below.

2 Conceptual Design Methodology

Aircraft design is the name given to the activities that span the creation on paper of a new flight vehicle. The design process is usually divided into three phases or levels of design [Leland]: **Conceptual Design ➔ Preliminary Design ➔ Detail Design.**

This methodology will only focus on conceptual design where the general configuration and size is determined. Parametric trade studies are conducted using preliminary estimates of aerodynamics and weight to converge on the best final configuration. The feasibility of the design to accomplish a given mission is established but the details of the configuration are not defined.

One will also consider only level flight. Whether it is intended to achieve surveillance at low altitude or serve as a high altitude communication platform, a solar aircraft capable of continuous flight needs to fly at constant altitude. In fact, the first one would be useless for ground surveillance at high altitude and the second one wouldn't cover a sufficient area at low altitude.

In this case, the energy and mass balances are the starting point of the design. In fact, the energy collected during the day by the solar panels has to be sufficient to power the motor, the onboard electronics and also charge the battery that provides enough power to fly from dusk to the next morning when a new cycle starts. Likewise, the lift force has to balance exactly the airplane weight so that the altitude is maintained.

This leads finally to an hen and egg problem: the required power consumption allows dimensioning the various parts, like motor, solar cells, battery, etc. but at the same time these parts determine the airplane gross weight used for the calculation of the required power. These relations are described in this section.

2.1 Irradiance model

A good model of irradiance depending on variables such as geographic position, time, solar panels orientation and albedo was developed based on [7]. For our need here, this model was simplified for flat surfaces by a sinusoid as shown on Fig. 2.

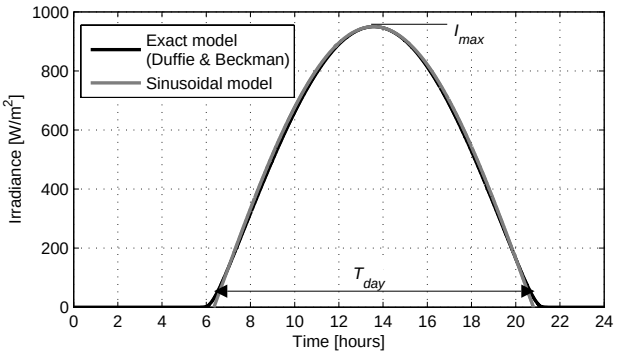

Fig. 2 Approximation of irradiance with a sinusoid (Lausanne, June 21)

The maximum irradiance I_{max} and the duration of the day T_{day}, which are depending on the location and the date, allows to compute the daily energy per square meter as depicted in Eq. 1. In order to take into account cloudy days, a constant is added with a value between 1 (clear sky) and 0 (dark). This constitutes a margin for the calculation.

$$E_{day\ density} = \frac{I_{\max} T_{day}}{\pi / 2} k_{solmargin} \quad \textbf{(1)}$$

2.2 Power balance for level flight

The forces acting on the airplane during level flight are the lift L and the drag D defined as:

$$L = C_L \frac{\rho}{2} S V^2 \qquad D = C_D \frac{\rho}{2} S V^2 \tag{2}$$

where C_L and C_D are respectively the lift and drag coefficients, ρ the air density, S the wing area and V the airplane relative speed which is similar to the ground speed if one assume no wind. C_L and C_D heavily depend on the airfoil, the angle of attack α, the *Re* number and *Mach* number. The drag coefficient is the sum of the airfoil drag C_{Da}, the parasitic drag of non-lifting parts that will be neglected here and the induced drag C_{Di} than can be estimated by:

$$C_{D_i} = \frac{C_L^{\,2}}{e\,\pi\,AR} \tag{3}$$

where e is the Oswald's efficiency factor and AR the aspect ratio of the wing, the ratio between the wingspan and the chord. From Eq. 2 one can find the power for level flight

$$P_{level} = \frac{C_D}{C_L^{3/2}} \sqrt{\frac{(m\,g)^3}{S}} \sqrt{\frac{2}{\rho}} \tag{4}$$

Using the relation between S, b and AR, one can rewrite:

$$P_{level} = \frac{C_D}{C_L^{3/2}} \sqrt{\frac{2\,AR\,g^3}{\rho}} \frac{m^{\frac{3}{2}}}{b} \tag{5}$$

Then, to obtain the total power consumption, efficiencies of the motor, its electronic controller, the gearbox and the propeller have to be taken into account, as well as the power consumption of the control and navigation system and the payload instruments. In order to lighten the reading, these relations will not be written here but further illustrated on Fig. 7.

2.3 Mass estimation models

For each part on the airplane, a good mass model is necessary in order to calculate the total mass m and use it in Eq. 5. The simple models will not be expressed in equation but only shortly described as they will be further illustrated in Fig. 7.

The mass of the control and navigation system is considered as fixed, just like the payload that is a requirement defined at the beginning. Concerning the battery, its mass is directly proportional to the energy it needs to store, which is the product between power consumption and night duration, and inversely proportional to its energy density.

In the case of the solar panels, one can find the area they cover by putting into equality the total electric energy consumed each day with the total electric energy obtained from the sun.

$$P_{elec\,tot}\left(T_{day} + \frac{T_{night}}{\eta_{chrg}\,\eta_{dischrg}}\right) = \frac{I_{\max}\,T_{day}}{\pi/2} k_{solmargin}\,A_{solar}\,\eta_{cells}\,\eta_{mppt} \tag{6}$$

The obtained area A_{solar} is then used to calculate the mass of the solar panels, taking into account the mass of the cells themselves and their encapsulation made of nonreflective sheets of polymer.

A special electronic device, called Maximum Power Point Tracker (MPPT) is required to adapt the voltage of the solar panels so that they provide the highest power possible. Its mass is proportional to the maximum power it has to convert, which can be calculated using the solar panels area calculated above as showed in equation Eq. 7. The constant k_{mppt} was found based on a study of existing high efficiency products (Fig. 3).

$$m_{mppt} = k_{mppt} P_{solmax} = k_{mppt} I_{\max} \eta_{cells} \eta_{mppt} A_{solar} \quad \textbf{(7)}$$

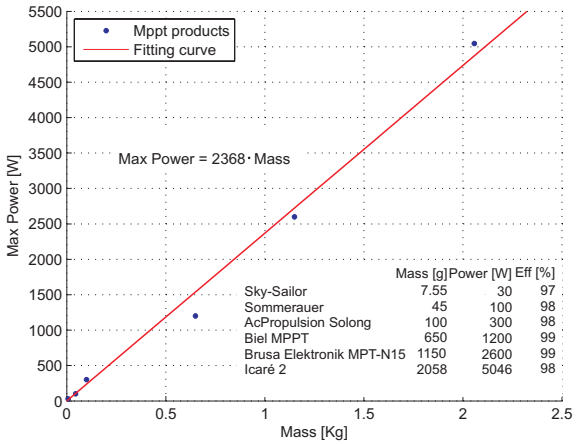

Fig. 3. Power density of high efficiency MPPTs

The mass of all the electric cables, especially those connecting the solar panels to the MPPT, can be modeled according to the airplane wingspan and the electrical current. However, in order to avoid a too complex model, this mass is included in the onboard electronics.

Concerning the propulsion group, composed of the motor, the gearbox and the propeller, [8] and [9] proposed a model, adapted from civil aircraft to solar airplane, which takes into account the number of blades, the propeller diameter and the power of the motor. Some calculations show that the estimation is far too optimistic for model aircraft. [18] and [25] propose very similar models exclusively based on power, where the mass of the propulsion group is estimated as

$$m_{prop} = 0.0045\, P_{prop} \quad \textbf{(8)}$$

For real large scale solar airplanes like *Helios, Icaré 2* or *Solair II*, this factor is respectively 0.0033, 0.0012 and 0.0008 kg/W whereas the first experiments with Sky-Sailor showed a factor of around 0.010 kg/W. The reason is that for an airplane taking off on a runway, the difference between start power and mean power for level flight is low. At the opposite, in the case of a hand launched model airplane that needs to increase its speed and take altitude rapidly, the start power is far higher than the mean power required for level flight. Thus, the motor has to be oversized and its mass increases.

Finally, the mass of the airplane structure is the most difficult part to model and the two main approaches mainly used in the literacy for solar airplanes appear inadequate. That is the reason why we will study this part more in details and propose a new model

The first approach from D.W. Hall [8] consists in calculating separately the mass of all the elements constituting the airframe, i.e the spar, the leading and trailing edge, covering, ribs, control surfaces, fuselage and tail as functions of the total mass, aspect ratio and wing area. It was applied by [6] on airplane with more than 60 m wingspan but shows to be inapplicable for model airplane. The second approach, proposed by W. Stender in 1969 [20], is based on statistical data for sailplanes with twin boom tails. The entire airframe weight is estimated parametrically as a function of aspect ratio, surface and number of boom tails.

$$W_{af} = 8.763\, n^{0.311}\, S^{0.778}\, AR^{0.467} \tag{9}$$

This simple model was adopted by [17], [18] and [25] for their solar airplane design. In order to verify this model, a database containing wingspan, wing area, aspect ratio, structure weight and gross weight of 415 sailplanes of various dimensions was created. They are divided into 92 radio controlled unmanned models and 323 manned sailplanes.

The weight of these samples is represented on Fig. 4 as function of the wing area and the aspect ratio. Eq. 9 is obviously very optimistic for large scale sailplanes and too pessimistic for model airplane. Thus, using a least-square fitting method, we propose a new equation based on the sailplane database described above.

$$W_{af} = 5.58\; S^{1.59}\, AR^{0.71} \tag{10}$$

Using the definition of aspect ratio, it can of course also be expressed as a function of wingspan:

$$W_{af} = 5.58 \cdot b^{3.18} \cdot AR^{-0.88} \tag{11}$$

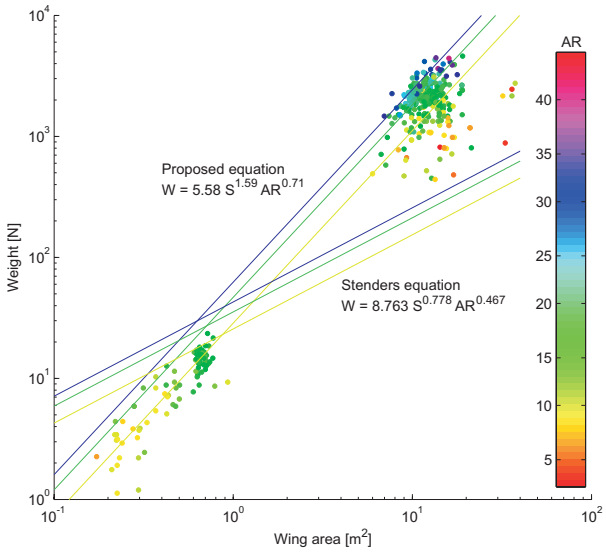

Fig. 4 Comparison of two airframe mass models with real data

But these equations only give the mean tendency of all the 415 records, in which the construction quality of airplane varies. As we are interested in having a model of the highest quality sailplanes only, we propose to separate the records in two groups, the one that have a lower weight than it would have been estimated by the interpolation and the others. Keeping only the first group and applying one more time the curve fitting process, we obtain after five iterations an equation that models the 5% best sailplanes

$$W_{af} = 0.44 \ S^{1.55} \ AR^{1.3} \quad \textbf{(12)}$$

Here again, one can rewrite Eq. 12 using wingspan instead of surface

$$W_{af} = 0.44 \cdot b^{3.1} \cdot AR^{-0.25} \quad \textbf{(13)}$$

It is interesting to see the evolution of the constant and the two exponents during the iterations when construction quality increases. The wing area is always related to the weight with a power of around 1.55 to 1.59, this exponent doesn't change significantly. At the opposite, the influence of the aspect ratio increases with the quality.

Several scientists studied the correlations between gross weight, wingspan, wing area and speed more generally including all the commercial flying machines, from the hang glider to the big airliners, and also in the animal kingdom, from the flies to the albatross. Above this amount of work, [19] offers an excellent and concise review of all these correlations.

One of the best contributors in this field is Henk Tennekes who presented very interesting correlations that he summarized in a log-log diagram named "The great flight diagram" [22]. The result is impressive: from the common fruit fly to the Boeing 747, all points follow approximately a line corresponding to Eq. 14.

$$W / S = 47 \cdot W^{1/3} \quad \textbf{(14)}$$

The concept of geometric similarity is the base of this equation; if one assumes geometric similarity among flying objects, the weight W is proportional to the cube of a characteristic length l, the surface S to the square and consequently the wing loading is linear with l and thus with $W^{1/3}$. It is interesting to notice that if we transform Eq. 12 that represents our model in the form above, the weight is linked to the wing loading with an exponent of 0.35 which is close to the model proposed by Tennekes.

$$W_{af} / S = 0.59 \cdot W_{af}^{\ 0.35} \cdot AR^{0.84} \quad \textbf{(15)}$$

Fig. 5 presents, superposed on the great flight diagram, the position of the 415 sailplanes as well as the mean and the top 5% model developed above. A model from B.W. McCormick [12] for the estimation of the wing loading of manned airplanes, also based on square-cubing scaling laws, is also represented. One remarkable point is its asymptote at a weight of 1000 N which corresponds to the weight of a single human person in an incredibly lightweight airplane. The airplane approaching the most this asymptote is the Gossamer Albatross, the human powered aircraft built by Dr. Mcready that crossed the English Channel in 1979.

Sixty-two of the most famous solar airplanes flown to date, from RC models to HALE platforms, are represented in the same way on Fig. 6. One can observe that whereas the small scale models are located in the same region than the non-solar one, the large scale solar airplanes are far away from the model we developed.

The reason is that Helios, Centurion, Pathfinder, Pathfinder Plus and Zephyr have a major difference in their configuration compared to all other models; in fact, their wing extremities are supported by several wheels, when not in flight. The flexion constraints on the wing are reduced which allows using a lighter construction method. These big models have impressive low weight but the direct consequence is their incredible fragility. That was the cause of Helios crash in 2003. The five manned solar airplanes are slightly above McCormick upper boundary, except Gossamer Penguin, the solar version of human powered Gossamer Albatross.

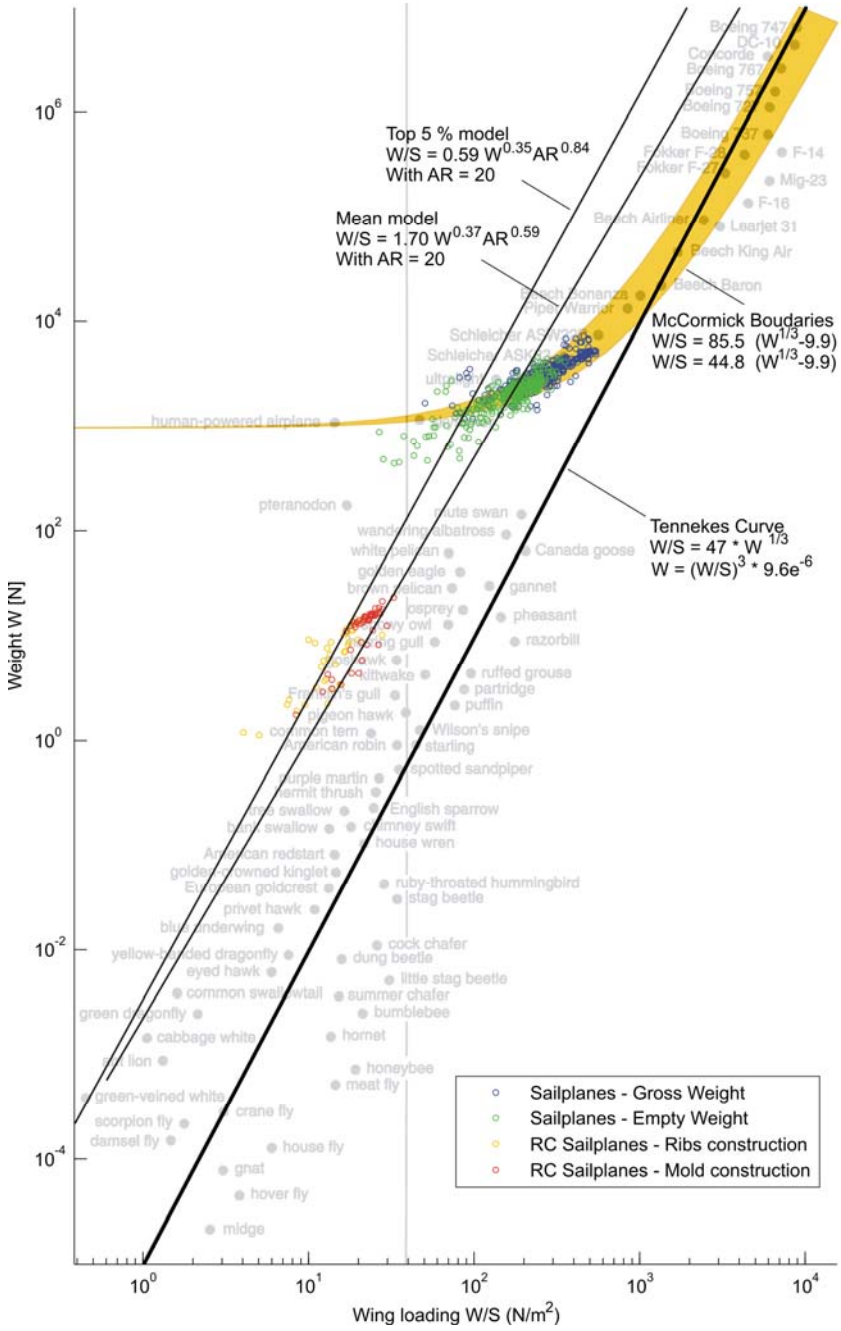

Fig. 5. The Great Flight Diagram [22] completed with 415 sailplanes

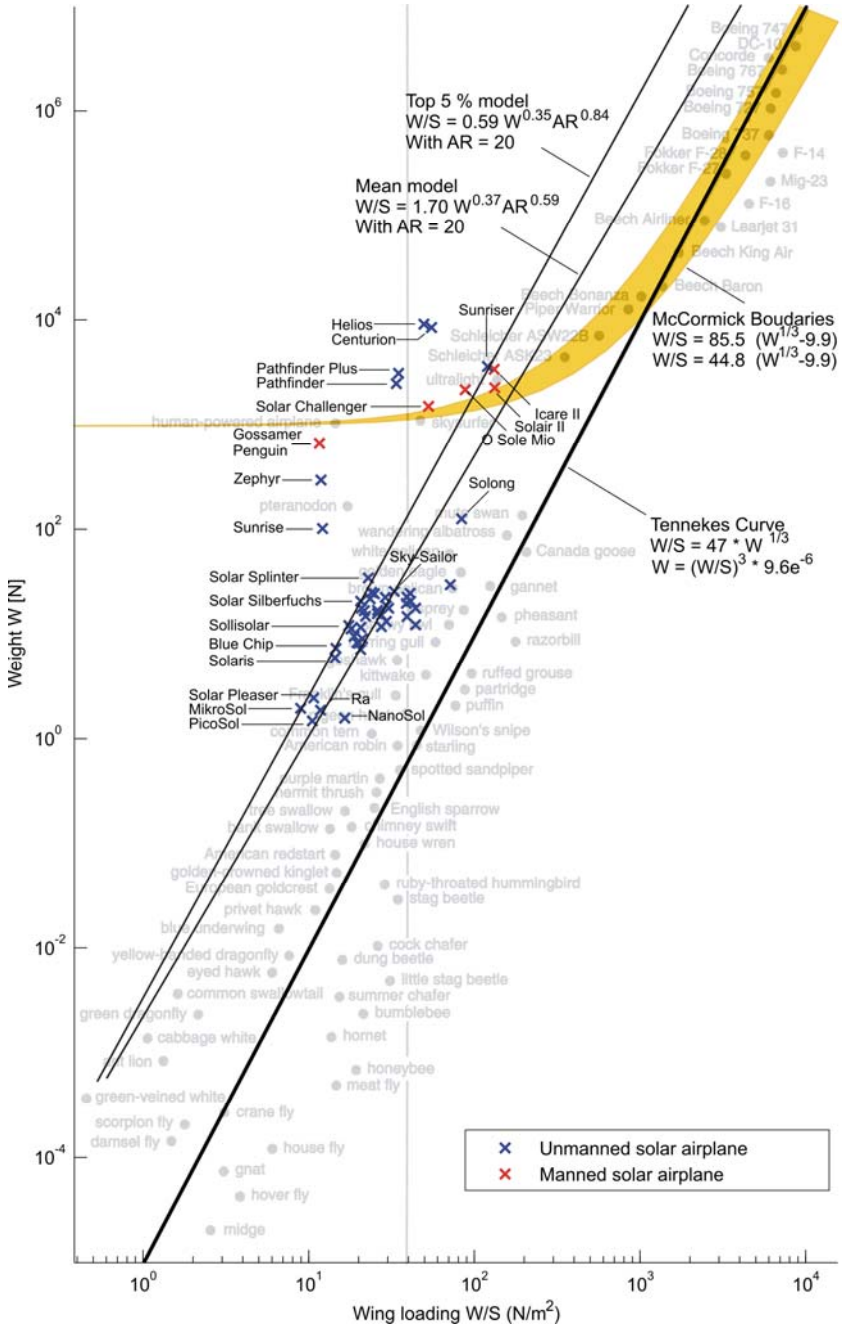

Fig. 6. The Great Flight Diagram [22] completed with 62 solar airplanes

2.4 Summary of the problem

A schematic representation of the power balance and the mass balance is shown on Fig. 7 where all the relations stated above are represented. In order to avoid the use of heavy equations in the following equations, the main expressions are replaced by variables a_0 to a_9.

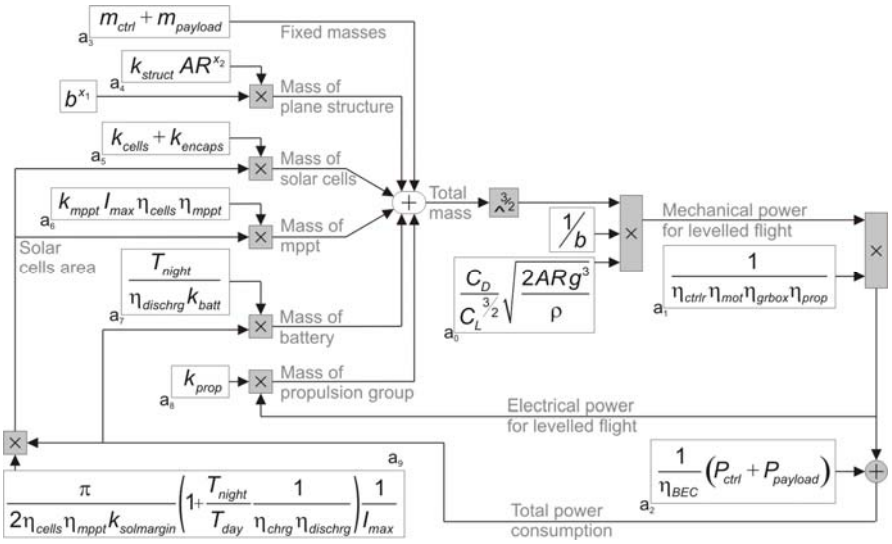

Fig. 7. Schematic representation of the design methodology

We are now able to solve this cyclic problem by using all these relations

$$m = m_{ctrl} + m_{payload} + m_{struct} + m_{solar} + m_{batt} + m_{mppt} + m_{prop} \tag{16}$$

$$m - \underbrace{a_0 a_1 \left(a_7 + a_8 + a_9\left(a_5 + a_6\right)\right)}_{a_{10}} \frac{1}{b} m^{\frac{3}{2}} = \underbrace{a_2\left(a_7 + a_9\left(a_5 + a_6\right)\right) + a_3}_{a_{11}} + a_4 b^{x_1} \tag{17}$$

Reducing one more time the complexity of the equation by using substitution variables, one obtains.

$$m - \underbrace{a_{10}\frac{1}{b}}_{a_{12}} m^{\frac{3}{2}} = \underbrace{a_{11} + a_4 b^{x_1}}_{a_{13}} \tag{18}$$

It can be shown that Eq. 19 has only a positive non-complex solution for *m*, which makes physically sense, if

$$a_{12}^2\, a_{13} \le \frac{4}{27} \tag{19}$$

For a given airplane configuration, the feasibility is proved if this inequality is respected and at the same time if the surface of solar cells is smaller than the wing area.

In order to be able to extract meaningful information, it is necessary, among the thirty parameters that our model contains, to distinguish between three different classes:

1. The first group is composed of the parameters which are linked to a technology and are constant or can be regarded as constant for very good design. This is for example the case of motor or propeller efficiencies that should be around 85 % when optimized for a special application.
2. The second group of parameters is linked to the type of mission; they concern flight altitude, date and payload.

3. Finally, the last group is composed of the parameters that we vary during the optimization process in order to determine the airplane layout, that is why one should use here the term variable that parameter. They are for example the wingspan or the aspect ratio.

A complete listing of these parameters is presented in the tables below. The values that are mentioned were used for the design of Sky-Sailor first prototype.

Table 1 Parameters that are constant or assumed constant

Parameter	Value	Unit	Description
C_L	0.8	-	Airfoil lift coefficient
C_{Da}	0.013	-	Airfoil drag coefficient
e	0.9	-	Oswald's efficiency factor
I_{max}	950	[W/m^2]	Maximum irradiance
k_{batt}	190·3600	[J/kg]	Energy density of battery
k_{cells}	0.32	[kg/m^2]	Mass density of solar cells
k_{encaps}	0.22	[kg/m^2]	Mass density of encapsulation
k_{mppt}	0.00047	[kg/W]	Mass to power ratio of mppt
k_{prop}	0.013	[kg/W]	Mass to power ratio of propulsion unit
k_{struct}	0.44/9.81	[kg/m^3]	Structural mass constant
m_{elec}	0.25	[kg]	Mass of navigation & control system
η_{bec}	0.7	-	Efficiency of step-down converter
η_{cells}	0.169	-	Efficiency of solar cells
η_{chrg}	0.98	-	Efficiency of battery charge
η_{ctrlr}	0.95	-	Efficiency of motor controller
$\eta_{dischrg}$	0.98	-	Efficiency of battery discharge
η_{grbox}	0.95	-	Efficiency of gearbox
η_{mot}	0.85	-	Efficiency of motor
η_{mppt}	0.97	-	Efficiency of mppt
η_{prop}	0.85	-	Efficiency of propeller
P_{ctrl}	1	[W]	Power of navigation & control system
x_1	3.1	-	Structural mass area exponent
x_2	-0.25	-	Structural mass aspect ratio exponent

Table 2 Parameters determined by the mission

Parameter	Value	Unit	Description
$k_{solmargin}$	0.7	-	Irradiance margin factor
$m_{payload}$	0.25	[kg]	Payload mass
$P_{payload}$	0.5	[W]	Payload power consumption
ρ	1.1655	[kg/m^3]	Air density (500 m)
T_{day}	14·3600	[s]	Day duration

Table 3 Variables linked to the airplane shape

Parameter	Value	Unit	Description
AR	12.9	-	Aspect ratio
b	3.2	[m]	Wingspan
m	2.6	[kg]	Total mass

3 Application of the methodology

Having the mission requirements, the method explained here above can be applied in order to evaluate the possible shapes of a solar airplane. This will be illustrated with the example of the Sky-Sailor prototype. The objective here is to embed a 250 g payload consuming 0.5 W and fly continuously at low altitude during two months in summer. These mission parameters allow plotting the relations between the main variables, i.e. wingspan and aspect ratio, and the flight characteristics for all the possible configurations.

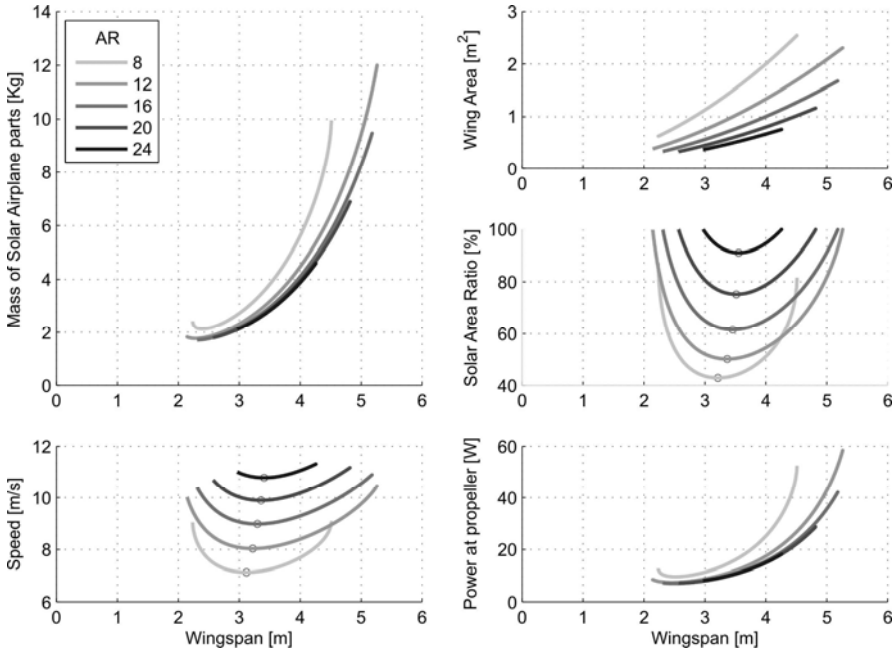

Fig. 8. Design plots of a solar airplane with a payload of 250 g

This is done on Fig. 8 where one can first observe that the minimum airplane wingspan is around 2.5 m and that keeping the same construction quality the airframe will become too heavy from a certain point and make continuous flight impossible. This means that for larger airplanes, the quality of the wing structure in terms of weight becomes more and more important. In the range of ten to twenty meters wingspan, which corresponds to commercial sailplanes, the construction method used today should be massively improved to see one day a model in this range fly continuously.

In our case, among the many possible configurations, the final choice will be guided by considerations on the flight speed, size or even production costs that can be estimated knowing the prices of the different elements.

It is also interesting to have a look on mass distribution. Fig 9 shows that the half of the weight is only due to the battery and that the structure constitutes also an important part that increases with wingspan as said before. This knowledge allows putting efforts on the critical parts instead of working on elements that play a minor role in overall mass.

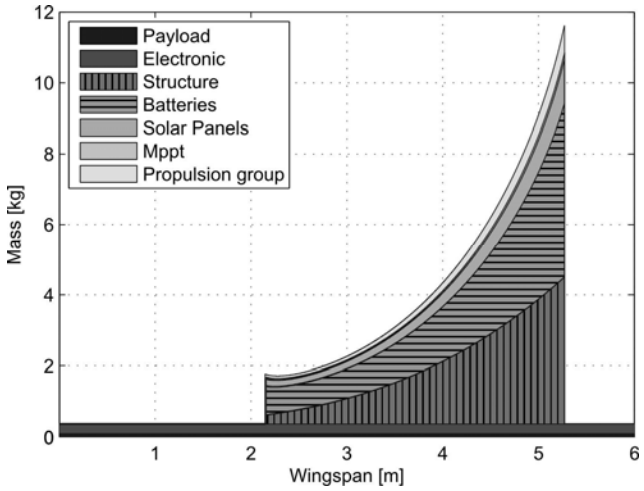

Fig. 9. Mass distribution with respect to wingspan assuming AR = 12

3.1 Influence of Technologies on the feasibility

By changing the value of parameters belonging to the first group of parameters listed in Table 1, one can evaluate what is the effect of technological changes or improvements. For example, concerning the choice of solar cells, one can compare the use of lightweight cells with low efficiency compared to heavier ones that are two times more efficient.

With the results that the methodology gives in the case of Sky-Sailor as explained in the previous chapter, one can see that the two major contributors in terms of weight are the battery and the wing structure. That is the reason why one will focus here on the two parts and observe the influence of the technology adopted.

Considerations about battery technology

Today, the highest energy ratio for rechargeable battery is around 200 Wh/kg for Lithium Polymer technology. But one can expect in some years an import increase of this value. The miniaturization of fuel cells will also make them suitable for small solar UAVs.

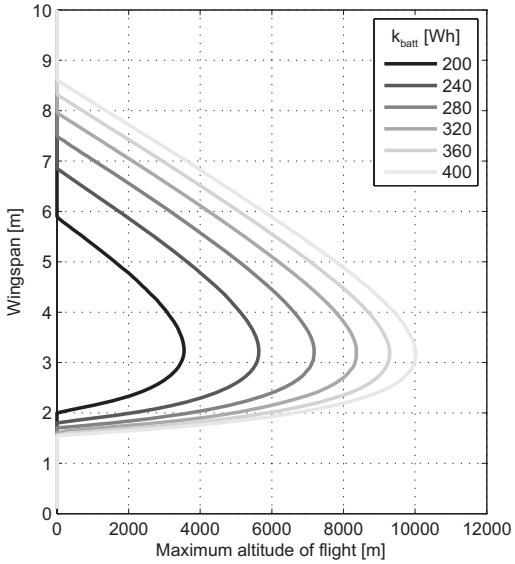

Fig. 10. Impact of the battery capacity on the flight altitude

Fig. 10 shows that in the case of Sky-Sailor, doubling the capacity of the energy storage system would make continuous flight at 10'000 m altitude possible.

Considerations about airplane structure

The application we saw with a payload of 0.5 kg showed us that continuous flight is possible for wingspan from 2.5 m to 5 m. Even in the scenario where no extra payload is embedded, these two limits exist. The reason is that using our cubic structural weight scaling law, the empty airframe becomes too heavy for high dimension. Hence, one can wonder what shape should this structural weight scaling law have to make continuous flight possible with all wingspan.

This is done, using our methodology, by setting k_{struct} to zero which means that we consider an ideal wing structure that has no mass. Then, try to know for a specified b and AR what the maximum payload weight that can be embedded is. Hence, this value will also be the maximum weight that the wing can have if we assume no payload. Starting with Eq. 19, we have:

$$a_{10}^2 \left(a_2 \left(a_7 + a_9 \left(a_5 + a_6\right)\right) + a_3\right)\frac{1}{b^2} \leq \frac{4}{27} \quad \textbf{(20)}$$

Then, isolating a_3 which corresponds to the payload mass, we have:

$$a_3 \leq \frac{4}{27a_{10}^2} b^2 - a_2 \left(a_7 + a_9 \left(a_5 + a_6\right)\right) \quad \textbf{(21)}$$

$$m_{payload} \leq \frac{4\,AR}{27a_{10}^2} S - a_2 \left(a_7 + a_9 \left(a_5 + a_6\right)\right) \quad \textbf{(22)}$$

One can then express the maximum admissible wing structure mass depending on its surface as depicted on Fig. 11.

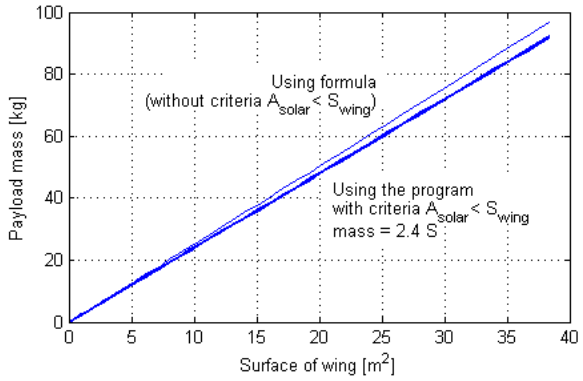

Fig. 11. Maximum admissible structure mass depending on wing surface for AR = 15

It is interesting to see that the relation is linear, which means that the ratio between mass and surface has to remain under a certain value. When plotting this relation on the Fig. 6, it proves clearly as it was said before that the realization of a solar airplane flying continuously is more difficult for higher wingspan. In fact, the top 5% model we identified has a surface density that increases whereas it should stay constant to guaranty feasibility.

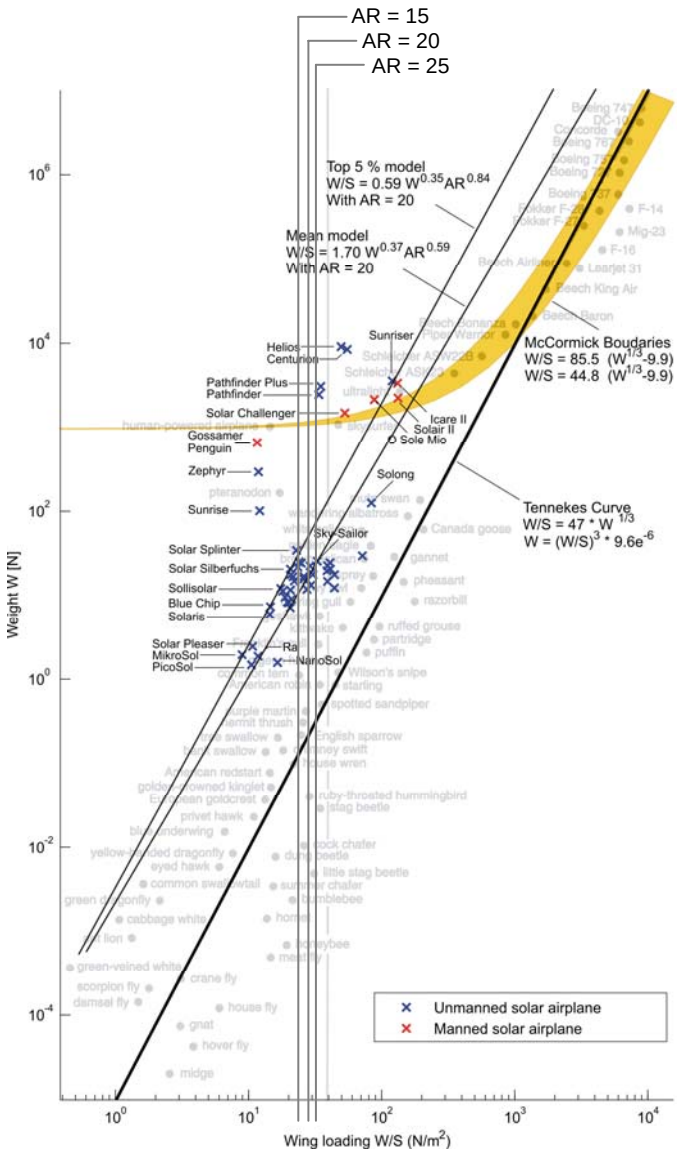

Fig. 12. Maximum admissible wing surface density

4 Conclusion

This lecture presented the global methodology that was developed for the design of the Sky-Sailor solar airplane. It was applied on our first prototype and revealed to be very useful, efficient and accurate [26]. The great benefit is that it is general enough to be applied to a wide range of size, from small model airplane to large scale high altitude platforms. Moreover, the analytical form of the method allows identifying clearly some general principles, like the constancy of wing surface density, the designer should be aware of. Hence, it was proved here that the realization of such airplane is more difficult for higher dimension. Of course, after this conceptual design phase, the next step is to achieve the preliminary design where the design of all the parts is approached more into details.

5 References

[1] Berry P (2000) The Sunriser - A Design Study in Solar Powered Flight, World Aviation Conference, San Diego, USA, Oct 10-12

[2] Boucher RJ (1984) History of Solar Flight, AIAA Paper 84-1429

[3] Bruss H (1991) Solar Modellflug Grundlagen, Enwicklung, Praxis, Verlag für Technik und handwerk, Baden-Baden

[4] Buccieri D, Mullhaupt P, Jiang Z, Bonvin D (2006) Velocity Scheduling Controller for a Nonholonomic Mobile Robot, IEEE Chinese Control Conference

[5] Colozza AJ (1990) Preliminary Design of a Long-Endurance Mars Aircraft, AIAA 26th Joint Propulsion Conference, AIAA 90-2000, Orlando, FL, July 16-18

[6] Colozza AJ (1994) Effect of Power System Technology and Mission Requirements on High Altitude Long Endurance Aircraft, NASA CR 194455, February 1994.

[7] Duffie JA, Beckman WA (1991) Solar Engineering of Thermal Processes, Second Edition. New York, Wiley-Interscience

[8] Hall DW, Hall SA (1984) Structural Sizing of a Solar Powered Aircraft, Lockheed Missiles and Space Company, NASA Contractor Report 172313

[9] Keidel B (2000) Auslegung und Simulation von hochfliegenden, dauerhaft stationierbaren Solardrohnen, PhD Thesis, Lehrstuhl für Flugmechanik und Flugregelung, Technische Universität München

[10] MacCready PB, Lissaman PBS, Morgan WR (1983) Sun-Powered Aircraft Designs, Journal of Aircraft, Vol. 20 No. 6, June 1983. pp. 487-493

[11] Mattio A (2006) Modeling and Control of the UAV Sky-Sailor, Master Project report, Ecole Polytechnique Fédérale de Lausanne, Switzerland

[12] McCormick BW (1995) Aerodynamics, Aeronautics and Flight Mechanics, John Wiley & Sons, Inc. New York

[13] Noth A, Engel W, Siegwart R (2005) Design of an Ultra-Lightweight Autonomous Solar Airplane for Continuous Flight, Proceeding of Field and Service Robotics, Port Douglas, Australia

[14] Noth A, Engel W, Siegwart R (2006) Flying Solo and Solar to Mars, published in IEEE Robotics and Automation Magazine, special issue on Unmanned Aerial Vehicles, Vol. 13, No. 3, September 2006, pps 44-52

[15] Patel C (2002) The Design and Fabrication of a Solar Powered Model Aircraft, B. Tech Thesis, Dept. of Aerospace Engineering, IIT Bombay

[16] Phillips WH (1980) Some Design Considerations for Solar-Powered Aircraft. NASA Technical Paper 1675

[17] Romeo G, Frulla G (2004) HELIPLAT: high altitude very-long endurance solar powered UAV for telecommunication and Earth observation applications, The Aeronautical Journal 108, 277–293

[18] Rizzo E, Frediani A (2004) A Model for Solar Powered Aircraft Preliminary Design, ICCES 04, vol. 1, pp. 39-54, Madeira, Portugal

[19] Shyy W, Berg M, Ljungqvist D (1999) Flapping and flexible wings for biological and micro air vehicles, Progress in Aerospace Science 35:455-506

[20] Stender W (1969) Sailplane Weight Estimation, Organisation Scientifique et Technique Internationale du vol a Voile

[21] Stinton D (2001) The Design of the Aeroplane, Second edition, Blackwell Science, Oxford, United Kingdom

[22] Tennekes H (1996) The Simple Science of Flight, From Insects to Jumbo Jets, MIT Press, Cambridge

[23] Tozer TC, Grace D, Thompson J and Baynham P (2000) UAVs and HAPs - Potential Convergence for Military Communications, IEE Colloquium on "Military Satellite Communications", 6th June 2000

[24] Voit-Nitschmann R (2001) Solar- und Elektroflugzeuge - Geschichte und Zukunft, Jahrbuch aus Lehre und Forschung der Universität Stuttgart, Online Jahrbuch 2001

[25] Youngblood JW, Talay TA, Pegg RJ (1984) Design of Long-Endurance Unmanned Airplanes Incorporating Solar and Fuel Cell Propulsion, AIAA/SAE/ASME 20th Joint Propulsion Conference

[26] http://www.asl.ethz.ch/research/asl/skysailor & http://sky-sailor.epfl.ch